



# Enhanced cycling performance of silicon/disordered carbon/carbon nanotubes composite for lithium ion batteries

Zhibin Zhou\*, Yunhua Xu, Mirabbos Hojamberdiev, Wengang Liu, Juan Wang

School of Materials Science and Engineering, Xi'an University of Architecture and Technology, 13 Yanta Road, Xi'an, Shaanxi 710055, PR China

## ARTICLE INFO

### Article history:

Received 16 March 2010  
Received in revised form 27 July 2010  
Accepted 27 July 2010  
Available online 4 August 2010

### Keywords:

Silicon  
Disordered carbon  
Carbon nanotubes  
Anode material

## ABSTRACT

A composite anode material of silicon/disordered carbon/carbon nanotubes (Si/DC/CNTs) was prepared by pyrolyzing the mixture of silicon (Si), carbon nanotubes (CNTs), and polyvinyl chloride (PVC) as carbon source. The X-ray diffraction (XRD) analysis confirmed that the phase transition of Si from crystalline to amorphous form occurred during the first cycle. The field-emission scanning electron microscopy (FESEM) observation revealed that Si particles wrapped by a CNTs network were homogeneously embedded into the carbonaceous matrix. The Si/DC/CNTs composite showed a discharge capacity of 1254 mAh/g in the first cycle, and a discharge capacity of 821 mAh/g after 20 cycles, which is much higher than that of Si/DC composite (658 mAh/g). It was found that the excellent resiliency of the CNTs can assist the carbonaceous matrix derived from PVC to restore the volumetric changes of the Si.

© 2010 Elsevier B.V. All rights reserved.

## 1. Introduction

Li-ion batteries have been intensively used in portable electronics, aerial devices, and electric automobiles because of their high specific capacity and excellent cycling performance. To develop the high capacity density anode materials for Li-ion batteries, considerable efforts have been made so far, especially focusing on Si as an anode due to its high theoretical capacity (4200 mAh/g) [1–3]. However, Si particles show a strong volumetric effect during the repeated alloying and dealloying process of Li with Si, which leads to poor cyclability [4,5]. A variety of composites containing silicon particles have been prepared to enhance the electrochemical properties of Si [6–10]. Among these composites, carbonaceous matrixes have shown more advantages over others [11–13], for example, silicon/disordered carbon [14], silicon/graphite [15], and silicon/graphene [16]. The DC materials can relieve and buffer the severe volumetric changes of silicon particles. So the Si/DC composites have exhibited even higher capacity and better cycling performance. However, it is still challenging to have high capacity and good cyclability simultaneously in the Si/DC composites. Because increasing the weight percentage of Si in the composite can give a high capacity but low cycling performance and decreasing the weight percentage of Si can give a good cyclability but low specific capacity. The unique properties of the CNTs, namely, superior mechanical strength and good electrical conductivity, improved the

electrochemical performance of the Si/C/CNTs composites significantly [17,18].

As reported previously, different carbon sources, namely, pitch [13], sugar [14], polyacrylonitrile [15], resorcinol [19], polyvinyl alcohol [20], and phenol-formaldehyde resin [21,22], had different effects on the enhancement of properties of the Si/DC composite. To the best of our knowledge, we first report the preparation of the Si/DC/CNTs composite using PVC as carbon source. The contribution of carbon source on the improvement of cycling performance of the Si/DC/CNTs composite is discussed in this work.

## 2. Experimental

The CNTs purchased from Chengdu Organic Chemical Co., China, have a diameter of 30–50 nm and length of about 1 μm. The particle size of silicon purchased from Hefei Kaier Nanotechnology Development Co., China, is about 80–100 nm. First, 1.5 g PVC was dissolved in 20 mL propylene oxide, and then 0.15 g Si and 0.13 g CNTs were separately dispersed in 20 mL propylene oxide using a high power ultrasonicator. The last two solutions were introduced drop-wise into the PVC solution and mixed by mechanical stirring to obtain a viscous residue at room temperature. The viscous residue was dried in a vacuum oven at 100 °C overnight, sealed in a quartz tube, heated at 900 °C under argon atmosphere for 2 h at a heating rate of 5 °C/min, and then cooled down to room temperature. Two parallel experiments were also conducted under the current conditions in the absence of CNTs and CNTs/Si. Silicon/disordered carbon/carbon nanotubes, silicon/disordered carbon, and disordered carbon were labeled as Si/DC/CNTs, Si/DC, and DC hereafter. The yield of the DC from PVC was calculated according to the weight loss before and after sintering in the quartz tube. The compositions of the Si/DC/CNTs and Si/DC nanocomposites were estimated on the basis of a yield of 10% from PVC to disordered carbon, and no weight loss for Si and CNTs.

X-ray powder diffraction (XRD) measurements were performed using a D/Max2400 diffractometer (Rigaku, Japan) with monochromated Cu Kα radiation to identify the phases. The morphology of the composite was examined by a field-emission scanning electron microscope (JSM-6700F, JEOL, Japan).

\* Corresponding author. Tel.: +86 29 82202718; fax: +86 29 82207898.  
E-mail address: [zhouzhibin.student@sina.com](mailto:zhouzhibin.student@sina.com) (Z. Zhou).

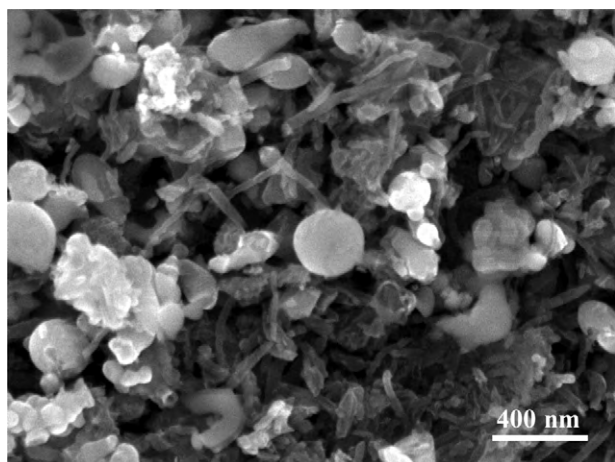


Fig. 1. FESEM micrograph of the Si/DC/CNTs composite.

The working electrodes were prepared by casting the slurry of sample powder (80 wt.%), acetylene black (5 wt.%), and polyvinylidene fluoride (PVDF, 15 wt.%) dissolved in *N*-methylpyrrolidone (NMP) on a copper foil, dried under vacuum at 120 °C overnight and pressed at 2 MPa for 10 s. Li foil was used as counter electrode. The working and counter electrodes were separated with a Celgard 2400 separator in an argon-filled glove box. 1 M LiPF<sub>6</sub> dissolved in the mixture of ethylene carbonate (EC) and diethyl carbonate (DEC) (1:1 in volume) was the electrolyte. The charge–discharge characteristics were obtained at room temperature between 0 V and 3 V at a constant current density of 30 mA/g.

### 3. Results and discussion

The SEM image of the Si/DC/CNTs composite before charge–discharge cycling performance is displayed in Fig. 1. As can be seen, the bright particles are nanocrystalline silicon, and the CNTs fibers are the connecting main wires to form a network that can finely wrap silicon particles. Si and CNTs are homogeneously distributed within the carbonaceous matrix, and the agglomeration of Si or CNTs is not observed.

The charge–discharge curves of the first, second, and tenth cycles of the Si/DC/CNTs composite are shown in Fig. 2. Clearly, during the first discharge process, a distinct plateau, corresponding to the formation of solid electrolyte interface film, can be observed at around 0.8 V, and this plateau disappears during the following cycles. Compared with the discharge curve of the first cycle, the discharge curve of the second cycle becomes more declining, and the voltage plateau ascends about 0.2 V than that of the first cycle.

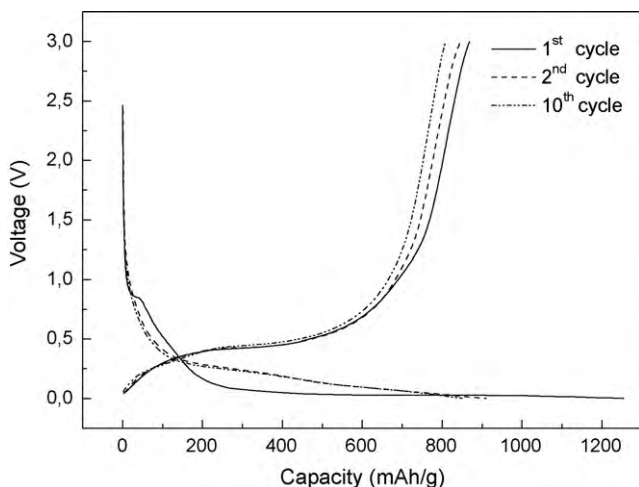


Fig. 2. Charge–discharge curves of the Si/DC/CNTs composite.

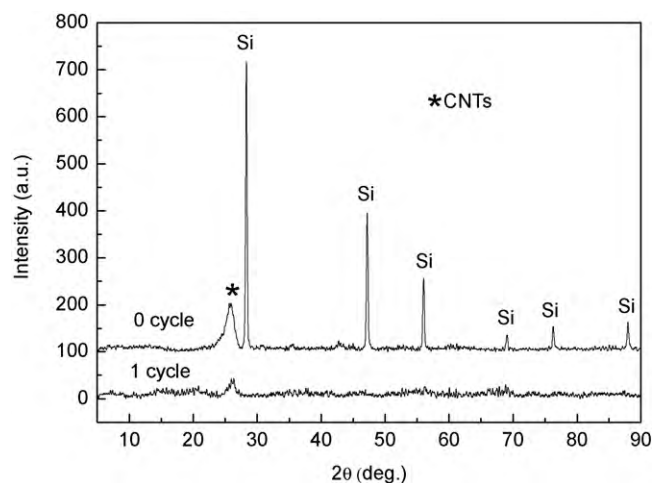


Fig. 3. XRD patterns of the Si/DC/CNTs composite.

The discharge curves of the subsequent cycles are almost consistent with that of the second cycle. The difference of the discharge curves between the initial and the subsequent cycles indicates that the phase structure transition of the composite might have occurred. The XRD measurements were performed to confirm phase structure transition of the Si/DC/CNTs composite. Fig. 3 shows the XRD patterns of the Si/DC/CNTs composite before and after lithium extraction. As shown in Fig. 3a, the diffraction peaks of Si with high intensity can be observed before cycling and no any diffraction peaks of inert SiC or SiO<sub>x</sub> are detected. The carbon derived from PVC shows no any significant diffraction peaks, indicating that the carbon in the composite is in the disordered state. As can be seen in Fig. 3b, the diffraction peaks of Si completely disappeared after lithium extraction. This is mainly attributed to the phase transition of Si from crystalline to amorphous form during the first cycle.

The cycling performances of the Si/DC/CNTs, Si/DC, Si, CNTs, and DC as anode materials are shown in Fig. 4. It can be seen that the pure Si shows a high capacity in the initial cycle, but the capacity drops down dramatically in the next cycles. The CNTs show a good cycling performance except for a high irreversible capacity in the first cycle, and a discharge capacity of 215 mAh/g retains after 20 charge–discharge cycles. Compared with CNTs, DC shows higher capacity and a discharge capacity of 350 mAh/g is obtained after 20 cycles. The Si/DC composite exhibits high capacity in the

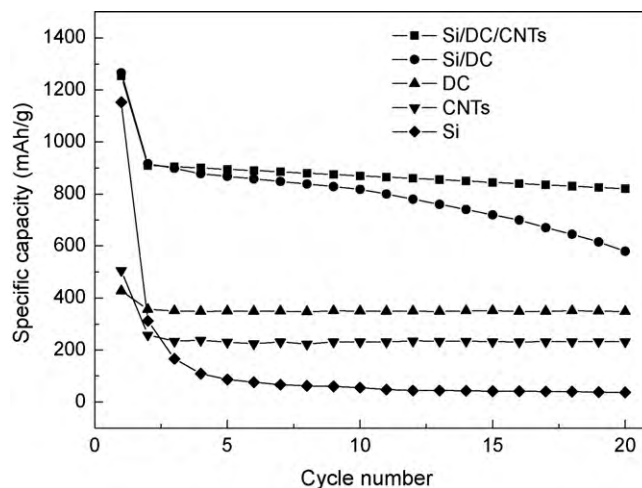


Fig. 4. Cycling performance of Si, DC, CNTs, Si/DC, and Si/DC/CNTs as anode materials.

first 10 cycles, but the discharge capacity of the Si/DC composite begins to drop rapidly after 10 cycles. After 20 cycles, only a discharge capacity of 658 mAh/g is retained. However, the Si/DC/CNTs composite not only show a high capacity, but also a good cycling performance. A discharge capacity of 1254 mAh/g is obtained in the first cycle, and a discharge capacity of 821 mAh/g is still retained after 20 cycles. To compare with that of the Si/DC composite, the cycling performance of the Si/DC/CNTs composite is enhanced remarkably.

In our experiment, the Si/DC/CNTs composite contains approximately 35 wt.% Si, 35 wt.% DC and 30 wt.% CNTs, and the Si/DC composite contains approximately 35 wt.% Si and 65 wt.% DC. As can be seen in Fig. 4, the discharge capacity of DC is much higher than that of CNTs. Compared with the Si/DC composite, the weight percentage of Si in the Si/DC/CNTs composite is identical, but the weight percentage of DC is lower. Hence, it can be speculated that the capacity of the Si/DC/CNTs composite should be lower than that of the Si/DC composite. However, the electrochemical testing shows that the capacity of the Si/DC/CNTs composite is nearly equally with that of the Si/DC composite during the initial cycles. The main reason may be explained that the good electrical conductivity of the CNTs can lead to more Si particles in the Si/DC/CNTs composite to be active with Li during the charge–discharge cycles. Though the Si/DC composite exhibits high capacity in the first several cycles, but drops down markedly in the subsequent cycles. This indicates that the DC matrix to absorb and buffer the large volume changes of Si during the alloying and dealloying process was still not enough. By adding CNTs into the Si/DC composite, CNTs form a network in the Si/DC/CNTs composite as electrical wires. The excellent resiliency of the CNTs can assist the DC matrix to restore the volumetric changes of the Si. So the effect of the carbonaceous matrix derived from PVC to relieve and buffer the volume change of Si is enhanced remarkably, which will ultimately lead to the stable structure of the electrode. In addition, the DC derived from PVC shows higher discharge capacity than that of the DC derived from the phenol-formaldehyde resin (PFR), which might be due to the higher specific surface area of the DC obtained from PVC [23]. So on the same weight percentage of DC, the Si/DC/CNTs composite using DC derived from PVC as carbonaceous matrix can possess a higher capacity.

#### 4. Conclusion

In this study, a novel composite anode material of Si/DC/CNTs was prepared using polyvinyl chloride (PVC) as carbon source. CNTs wrapping the Si particles form a network structure in the carbonaceous matrix. Compared with the Si/DC composite, the cycle performance of the Si/DC/CNTs composite was improved significantly. A discharge capacity of 821 mAh/g was retained after 20 charge–discharge cycles. The excellent resiliency and good electrical conductivity of the CNTs can keep more Si particles electrochemically active with Li and more stable morphology of the Si/DC/CNTs composite during the charge–discharge cycles.

#### References

- [1] V. Baranchugov, E. Markevich, E. Pollak, G. Salitra, D. Aurbach, *Electrochem. Commun.* 9 (2007) 796.
- [2] K. Ameszawa, N. Yamamoto, Y. Tomii, Y. Ito, *J. Electrochem. Soc.* 145 (1998) 1986.
- [3] S. Bourderau, T. Brousse, D.M. Schleich, *J. Power Sources* 81–82 (1999) 233.
- [4] J. Yang, M. Winter, J.O. Besenhard, *Solid State Ionics* 90 (1996) 281.
- [5] J.O. Besenhard, J. Yang, M. Winter, *J. Power Sources* 68 (1997) 87.
- [6] M.K. Datta, P.N. Kumta, *J. Power Sources* 165 (2007) 368.
- [7] N. Dimov, S. Kugino, M. Yoshio, *J. Power Sources* 136 (2004) 108.
- [8] V.G. Khomeenko, V.Z. Barsukov, J.E. Doninger, I.V. Barsukov, *J. Power Sources* 165 (2007) 598.
- [9] N. Dimov, M. Yoshio, *J. Power Sources* 174 (2007) 607–612.
- [10] Y.S. Jung, K.T. Lee, S.M. Oh, *Electrochim. Acta* 52 (2007) 7061.
- [11] W. Xing, A.M. Wilson, G. Zank, J.R. Dahn, *Solid State Ionics* 93 (1997) 239.
- [12] M. Yoshio, H. Wang, K. Fukuda, T. Umeno, N. Dimov, Z. Ogumi, *J. Electrochem. Soc.* 149 (2002) A1598.
- [13] Z.S. Wen, J. Yang, B.F. Wang, K. Wang, Y. Liu, *Electrochem. Commun.* 5 (2003) 165.
- [14] Z.P. Guo, E. Milin, J.Z. Wang, J. Chen, H.K. Liu, *J. Electrochem. Soc.* 152 (2005) A2211.
- [15] M.K. Datta, P.N. Kumta, *J. Power Sources* 158 (2006) 557.
- [16] S.-L. Chou, J.-Z. Wang, M. Choucair, H.-K. Liu, J.A. Stride, S.-X. Dou, *Electrochem. Commun.* 12 (2010) 303.
- [17] A. Thess, R. Lee, P. Nikolaev, H. Dai, P. Petit, J. Robert, C. Xu, Y.H. Lee, S.G. Kim, A.G. Rinzler, D.T. Colbert, G. Scuseria, D. Tománek, J.E. Fischer, R.E. Smalley, *Science* 273 (1996) 483.
- [18] M.M.J. Treacy, T.W. Ebbesen, J.M. Gibson, *Nature* 381 (1996) 678.
- [19] G.X. Wang, J.H. Ahn, J. Yao, S. Bewlay, H.K. Liu, *Electrochem. Commun.* 6 (2004) 689.
- [20] Z.P. Guo, D.Z. Jia, L. Yuan, H.K. Liu, *J. Power Sources* 159 (2006) 332.
- [21] Z.B. Zhou, Y.H. Xu, W.G. Liu, L.B. Niu, *J. Alloys Compd.* 493 (2010) 636.
- [22] P.J. Zuo, G.P. Yin, Y.L. Ma, *Electrochim. Acta* 15 (2007) 4878.
- [23] J.B. Gong, H.Q. Wu, Q.H. Yang, *Carbon* 37 (1999) 1409.